

Applied Mathematics and Nonlinear Sciences

<https://www.sciendo.com>

Mechanical behaviour of continuous girder bridge with corrugated steel webs constructed by RW

Bai Zhiping¹, Cheng Qian^{2†}, Wang Zhangming³, Liu Tiancheng², An Jin⁴

¹ Inner Mongolia Senior Highway Construction and Development Co., Ltd., Huhhot 010051

² CCCC Highway Bridges National Engineering Research Centre, Ltd., Beijing 100088

³ School of Civil Engineering, Beijing Jiaotong University, Beijing 100044

⁴ Shanghai Interlink Road & Bridge Engineering Co., Ltd., Shanghai 201315

Submission Info

Communicated by Juan Luis García Guirao

Received October 23rd 2021

Accepted November 27th 2021

Available online April 29th 2022

Abstract

Rapid construction of ripple web (RW) is a new construction technology that can be applied to the prestressed concrete (PC) box girder bridge with corrugated steel webs (CSWs). In order to analyse the mechanical behaviour in the construction process when the RW method is applied, the main bridge of Zhao-Jun Yellow River Super Large Bridge was adapted as the engineering background, and a three-dimensional simulation finite element model was established. Thereafter, detailed mechanical analyses were carried out for CSWs, top concrete and bottom concrete, lining concrete, temporary support and other structures in the construction process when the RW method was used. The results reveal the excellent quality of the mechanical properties of the structure, thus indicating the structure's safety and reliability. This study can provide a reference for similar research and have a positive impact on the further promotion of the RW method for application in the continuous girder bridge with CSWs.

Keywords: rapid construction of ripple web, corrugated steel webs, continuous girder bridge, construction technology, finite numerical method

1 Introduction

The pre-stressed concrete (PC) box girder bridge with corrugated steel webs (CSWs) is a new structure, which consists of top concrete and bottom concrete, CSWs, diaphragm plate and internal or external tendon [1, 2]. The PC girder bridge with CSWs adopts the CSWs instead of normal concrete webs, providing light weight, good seismic performance, convenient construction, economical construction management and several

[†]Corresponding author.

Email address: chengqian@bnerc.com

other significant advantages. This new type of structure can remove the concrete web cracking and excessive deflection in the mid-span in a large-span continuous beam or continuous rigid frame bridge, and thus improve the durability of the structure. Since the Guangshan Pohe Bridge, the first road bridge with CSWs, was built in 2005, this structure has been used in Henan Weihe Bridge (2010), Jiangxi Chaoyang Bridge (2012), Shanxi Yunbao Yellow River Bridge (2018) and many other places besides [3].

The box girder bridge with CSWs uses a construction technology that is similar to that of the normal concrete box girder bridge, including full framing method, incremental launching method and cantilever casting method. Among them, the full framing method is suitable for construction of small span bridge, and the incremental launching method for construction of medium span bridge with equal height section. For large-span CSW composite box girder bridge with variable section, the cantilever casting method is generally adopted. Motivated by the availability of advanced technology, engineers propose a new construction technology – rapid construction of ripple web (RW), which can be combined with the cantilever casting method. This construction technology originated in Japan, and has been used in more than 30 bridges, including the Tsukumi River Bridge and Kinugawa River Bridge. The optimal performance of these bridges demonstrates the effectiveness of this construction method. Till date, the RW method has been used in the construction of Yunbao Yellow River Bridge and Toudao River Bridge in China.

Ning et al. [4] have discussed the applicability of the RW method in the construction of a continuous girder bridge with CSWs by analysing the means by which this method was applied in the construction of Yunbao Yellow River Bridge, and proposed a limit division of a 4.8 m construction segment. Hui et al. [5] have developed a new type of hanging basket that is suitable for bridges with CSWs, and is in agreement with the structural characteristics of the box girder bridge with CSWs and the construction technology of the RW method. Besides, Mingjun [6] has analysed the normal stress of the top concrete and bottom concrete and the shear stress of the steel webs when the RW construction method was used, and verified the safety of structures constructed using RW. Several bridges constructed using the RW method have shown consistent good performance, demonstrating the advantages of this method; however, the stress status of the steel-concrete junction area is still very complicated during the construction process. Moreover, only very few researches have been carried out ascertaining the reliability of the connection of the shear connector used in the steel-concrete junction area and regarding cracking of the concrete tension area. In this paper, a three-dimensional simulation finite element model was established based on the Zhao-Jun Yellow River Super Large Bridge to discuss the space mechanical behaviour of the bridge with CSWs constructed by the RW method. The present study can be used as a reference for following applications deploying such new construction technology.

2 Project Overview

The construction of the Zhao-Jun Yellow River Super Large Bridge has contributed to the accumulation of more construction experience in relation to the girder bridge with CSWs in China, because this bridge was built using the new RW method and fully uses the stress characteristics of CSWs. During the construction process, a new hanging basket was used to apply the RW method for the construction of top concrete and bottom concrete. Compared with the rhombic hanging basket, the new means for construction of top concrete and bottom concrete by the RW method provides higher efficiency, greatly shortening the construction period. The main bridge of Zhao-Jun Yellow River Super Large Bridge is expected to be completed by the end of 2021.

2.1 Structure Overview

The main bridge of Zhao-Jun Yellow River Super Large Bridge is 1,520 m long, with the span combination of 85 m + 9 × 150 m + 85 m. At present, it is the longest continuous girder bridge designed with long spans and CSWs in China. The single width girder is designed with single-box and single-cell slabbing webs, and the left and right width box girders are symmetrical about the centre line of the bridge. The top slab of the single

width box girder is 12.75 m wide and 6.75 m wide for the bottom slab. In terms of height, the midspan girder is 5 m and the root girder is 10 m. They transit according to the 1.8-times parabola, and the schematic diagram of the half-span (1/2 span) box girder is shown in Figure 1. The main bridge's box girder adopts a longitudinal and transverse bidirectional prestressed system, and the longitudinal prestressed system of the box girder features a combination of internal and external stresses.

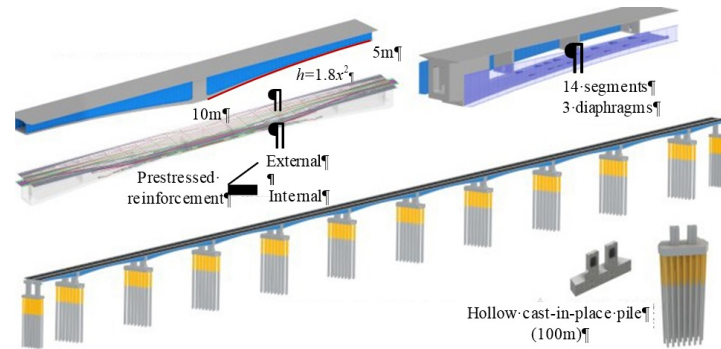


Fig. 1 Three-dimensional diagram of the prestressed concrete continuous girder with CSWs of Zhao-Jun Yellow River Super Large Bridge. CSW, corrugated steel webs

The wave length, wave height and width of the upper structure of the main bridge of Zhao-Jun Yellow River Super Large Bridge are 1.60 m, 0.22 m and 0.43 m, respectively. The horizontal folding angle is 30.7° and the bending radius is $15t$ (t is the thickness of the CSW). The CSWs have five thicknesses, namely 16 mm, 20 mm, 22 mm, 25 mm and 28 mm. The standard wave length of CSW is shown in Figure 2.

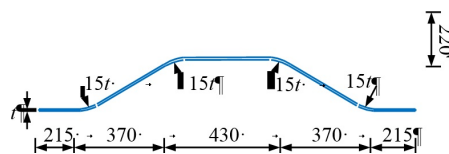


Fig. 2 Standard wavelength diagram of CSWs (in millimetres). CSW, corrugated steel webs

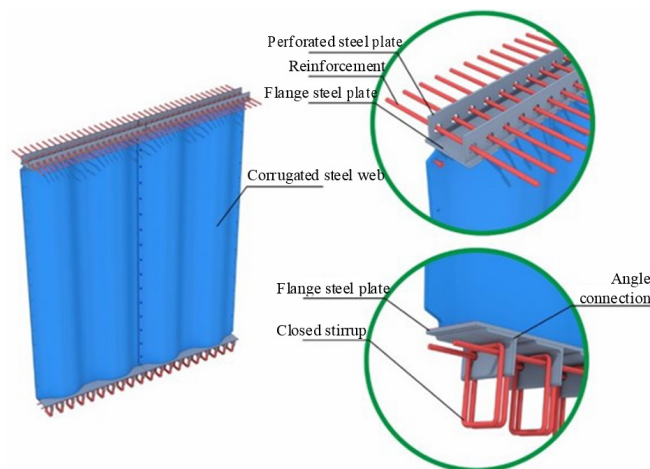


Fig. 3 Connection structure of the main bridge of Zhao-Jun Yellow River Super Large Bridge with CSWs. An inverted 'π' perforated steel plate is welded on the working areas, namely the $n-1$, $n\#$ and $n+1\#$ segment working areas. CSW, corrugated steel webs

The CSWs are connected with top concrete by double perfobond rib shear connectors (PBL) at the top of the CSW, which is 25 mm thick and 420 mm wide. It can also be used as the bottom mould for pouring concrete at haunches of box girder. The CSW is connected with the bottom concrete by a 400 mm wide L-shaped 200 × 200 × 18 angle steel. The lower flange steel plate is 22 mm thick, and the angle steel is provided every 0.32 m in the direction of the longitudinal bridge. The connection structure of the main bridge of Zhao-Jun Yellow River Super Large Bridge with CSWs is shown in Figure 3.

2.2 Construction by RW Method

As shown in Figure 4, when the PC composite box girder bridge with CSWs is constructed by the traditional hanging basket method, the installation of CSWs, formwork, reinforcement binding of top concrete and bottom concrete and concrete casting in the working area can only be carried out at the $n\#$ segment working face, after the hanging basket is installed in place. It only provides a limited working area where many cross operations must be done, thus leading to a longer construction period. However, when the RW method is adopted for pouring construction, the working area is expanded from a single working area to three. These areas are utilised in the following way: top concrete construction can be performed at $n\#$ segment working area, bottom concrete construction at $n-1\#$ segment working area and installation of CSWs at $n+1\#$ segment working area. This can greatly improve the construction efficiency, thus allowing a shorter construction period.

It is worth noting that in the construction process of cantilever casting by the RW method, the position of the basket fulcrum moves forward to the $n\#$ segment of the CSWs of the cantilever, which has not yet formed a closed box. In this way, the action arm of the cast girder body is lengthened and the bottom concrete and top concrete weight of one segment are added. Therefore, the inverted ‘ π ’ structure (top concrete not formed) at the $n-1\#$ segment and the box structure at the $n-2\#$ segment need to bear a large bending moment.

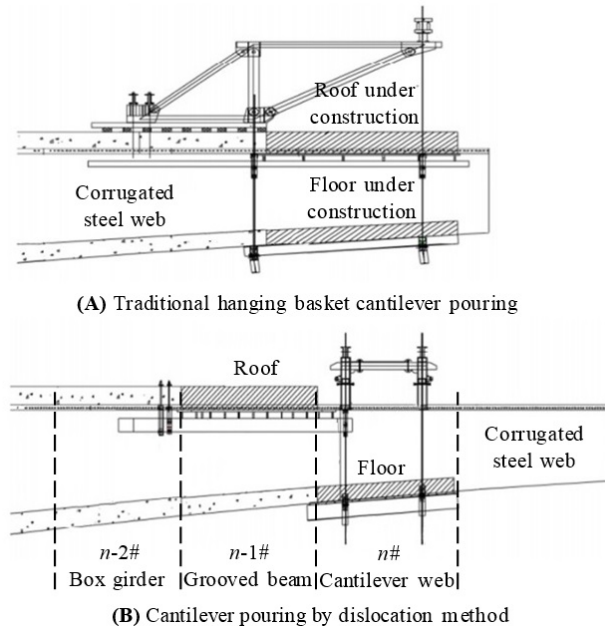


Fig. 4 Contrast diagram of cantilever casting process by ripple web

3 Finite Element Simulative Analysis

3.1 Structure analogue simulation

A three-dimensional solid element was used to cause the structure to reasonably and effectively simulate the actual structure of the bridge and the RW construction technology for top concrete and bottom concrete. A fine finite element analysis model of PC composite box girder with CSWs was established using ANSYS, a software of finite element analysis for parallel calculation analysis and comparative review of spatial linear elastic stress. The finite element model of mid-span structure is shown in Figure 5.

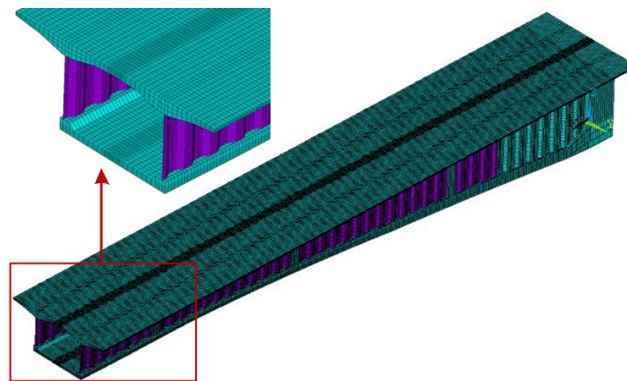


Fig. 5 Schematic diagram of finite element model of main mid-span structure

In the model, the concrete part adopted an 8-node hexahedral solid element, Solid65; and the CSWs' part adopted the plate shell element, Shell63. As shown in Figure 4(A), in the solid model of mid-span of Zhao-Jun Bridge, there are 126,512 nodes and 85,592 elements in the whole bridge. In this model, the prestressed steel bars were simulated by using the node coupling method, without considering the ordinary steel bar, the prestressed reduction and the transverse and longitudinal bending of the prestressed pipe. So, the pre-stressed steel bar was 1,395MPa.

The upper and lower flange plates of the CSWs were coupled with the top concrete and bottom concrete at the junction. Given that block 0# was in a consolidated state during the construction process, all degrees of freedom of nodes at the end of the girder were constrained in the model. The flange steel plates of CSWs were connected with concrete co-nodes.

Due to the small area of top concrete, the adoption of node-coupling method for pre-stressing loads will affect the junction of CSWs and concrete. As the stress generated when the prestressed steel is anchored into the concrete is concentrated, the excessive value will disturb the display effect of stress in the concerned area. Besides, the prestressed steel bars in the top concrete are used to avoid the tension of top concrete. Based on the above three considerations, the first principal stress of 0# concrete (cantilever root) was verified after the pre-stress was applied in all construction conditions. If it meets the requirements, the prestressed steel bar is removed, and the stress of CSW and the local stress of tensile top concrete and compressive bottom concrete are emphasised.

3.2 Construction process simulation

In the process of cantilever construction, the built old structure will displace vertically to deviate from the original coordinate position under the action of dead weight and various construction loads. The construction of steel structure requires that the newly installed segment and the installed node should be installed at the interface position to match exactly, corresponding to the tangent pattern in the diagram. When the new component is activated, the corner of the node is considered, and the new component used to simulate the construction step

is situated tangentially to the end of the deformed component. During the construction of concrete segments, the position of the subsequent segment formwork is often dynamically adjusted, corresponding to the model modification mode in the figure.

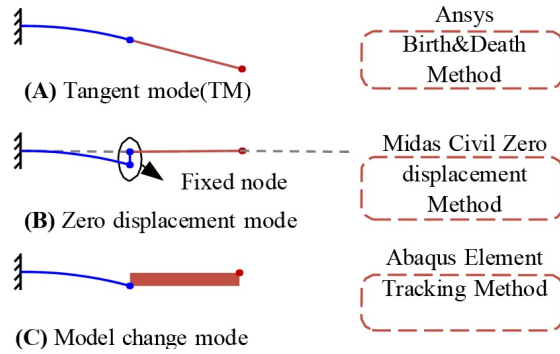


Fig. 6 Schematic diagram of finite element model of main mid-span structure

The ANSYS construction process simulation adopted the ‘Element Birth and Death’ [8, 9]. The method of Element Birth and Death is the integration of the formal analysis method on the finite element level. According to the proposed construction sequence, the corresponding construction phase of the component (or element) is ‘activated’, and the corresponding load is applied, after which the simulation analysis of the whole construction process can be tracked.

The Death Element is obtained by multiplying the stiffness and mass matrix of the inactive element by a small coefficient; the Death Element follows the boundary of the Birth Element. However, for large complex structures involving a closed loop, the Death Element often drifts too much, causing the structural configuration to be in a distorted state when the element is activated, which is inconsistent with the unstressed state. Also, the stiffness matrix of the structure is excessively ill-conditioned, leading to the failure of the solution.

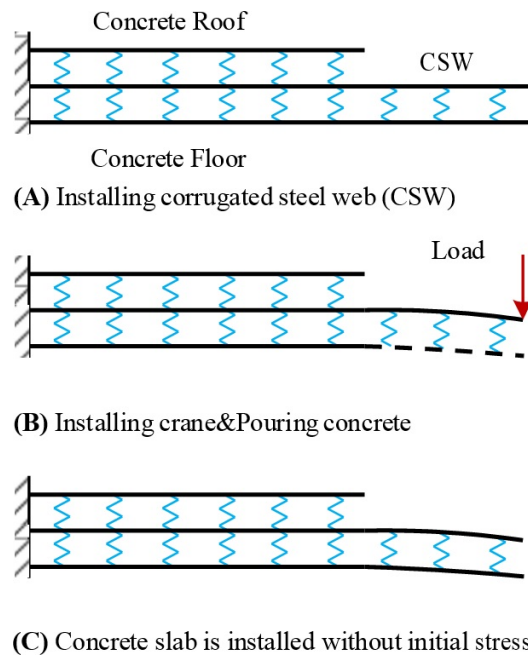


Fig. 7 Mechanism of 1/2 Element Birth and Death method in construction using ripple web

Figure 7 shows an example of construction of CSWs using RW. By the traditional step-by-step modelling method, several finite element models are required to be established at different construction stages. However, the Element Birth and Death method pays more attention to the influence on subsequent results after the completion of the previous stage in the construction process. As can be inferred from Figure 7(B), after the construction of concrete load on the crane, all the load falls on the CSWs, which will definitely cause vertical deflection of the CSWs of the cantilever. At this time, the poured concrete will be installed on the corresponding position without stress, along with the deformed CSWs. The principle of the step-by-step modelling method is as follows:

$$\begin{bmatrix} \mathbf{K}_{11}^{(1)} & \mathbf{K}_{12}^{(1)} \\ \mathbf{K}_{21}^{(1)} & \mathbf{K}_{22}^{(1)} + \mathbf{K}_{11}^{(2)} & \mathbf{K}_{12}^{(2)} \\ & \mathbf{K}_{21}^{(2)} & \mathbf{K}_{22}^{(2)} \end{bmatrix} \begin{bmatrix} \mathbf{u}_1 \\ \mathbf{u}_2 \\ \mathbf{u}_3 \end{bmatrix} = \begin{bmatrix} \mathbf{F}_1 \\ \mathbf{F}_2 \\ \mathbf{F}_3 \end{bmatrix} \tag{1}$$

Among them, $\mathbf{K}_{21}^{(2)}$ represents the \mathbf{K}_{21} matrix in element 2 (– i.e., the internal force value generated at node 2 when element displacement occurs at node 1).

When the Element Birth and Death method is adopted, the killed element is multiplied by a small coefficient η and the load on the element is deleted, and then Eq. (1) can be changed into Eq. (2):

$$\begin{bmatrix} \mathbf{K}_{11}^{(1)} & \mathbf{K}_{12}^{(1)} \\ \mathbf{K}_{21}^{(1)} & \mathbf{K}_{22}^{(1)} + \eta \mathbf{K}_{11}^{(2)} & \eta \mathbf{K}_{12}^{(2)} \\ & \eta \mathbf{K}_{21}^{(2)} & \eta \mathbf{K}_{22}^{(2)} \end{bmatrix} \begin{bmatrix} \mathbf{u}_1 \\ \mathbf{u}_2 \\ \mathbf{u}_3 \end{bmatrix} = \begin{bmatrix} \mathbf{F}_1 \\ \mathbf{F}_2 \\ 0 \end{bmatrix} \tag{2}$$

$$\begin{bmatrix} \mathbf{K}_{11}^{(1)} & \mathbf{K}_{12}^{(1)} \\ \mathbf{K}_{21}^{(1)} & \mathbf{K}_{22}^{(1)} \end{bmatrix} \begin{bmatrix} \mathbf{u}_1 \\ \mathbf{u}_2 \end{bmatrix} = \begin{bmatrix} \mathbf{F}_1 \\ \mathbf{F}_2 \end{bmatrix} \tag{3}$$

Eq. (2) can solve the activated element according to Eq. (3) first. At this time, the killed element exists in the form of the equation $\mathbf{K}_{21}^{(2)} \mathbf{u}_2 + \mathbf{K}_{22}^{(2)} \mathbf{u}_3 = 0$, which can be solved to obtain $\mathbf{u}_3 = \frac{\mathbf{K}_{21}^{(2)} \mathbf{u}_2}{\mathbf{K}_{22}^{(2)}}$. After all the displacements are obtained, the next construction stage begins. However, if the geometric nonlinearity caused by deformation is not considered, it is unnecessary to update the stiffness matrix, and the displacement matrix and load matrix of the new stage are marked with ‘’. The relevant equation will be the following:

$$\begin{bmatrix} \mathbf{K}_{11}^{(2)} & \mathbf{K}_{12}^{(2)} \\ \mathbf{K}_{21}^{(2)} & \mathbf{K}_{22}^{(2)} \end{bmatrix} \begin{bmatrix} \mathbf{u}'_2 \\ \mathbf{u}'_3 \end{bmatrix} = \begin{bmatrix} \mathbf{F}'_2 \\ \mathbf{F}'_3 \end{bmatrix} \tag{4}$$

where $\mathbf{u}'_2 = \mathbf{u}_2$ and $\mathbf{F}'_3 = \mathbf{F}_3$. After expanding the equation, we can get:

$$\mathbf{K}_{21}^{(2)} \mathbf{u}_2 + \mathbf{K}_{22}^{(2)} \mathbf{u}'_3 = \mathbf{F}'_3 \tag{5}$$

$$\mathbf{u}'_3 = \frac{\mathbf{F}'_3 - \mathbf{K}_{21}^{(2)} \mathbf{u}_2}{\mathbf{K}_{22}^{(2)}} \tag{6}$$

$$\mathbf{F}'_2 = \mathbf{K}_{11}^{(2)} \mathbf{u}_2 + \mathbf{K}_{12}^{(2)} \frac{\mathbf{F}'_3 - \mathbf{K}_{21}^{(2)} \mathbf{u}_2}{\mathbf{K}_{22}^{(2)}} \tag{7}$$

It is obvious that there is a mechanical relationship between the second construction stage and the previous construction stage. Therefore, the Element Birth and Death method can make the simulation of construction processes more suitable for the actual project.

4 Results and Analysis

According to the reaction force of the support from the separate calculation of the hanging basket, as shown in the table, it was substituted into the finite element simulation model reversely and the calculation results were given based on the working condition of the cantilever (2# top and 3# bottom concrete pouring). The structure load is: box girder weight + basket support reaction.

4.1 Stress Analysis of CSWs

Under the condition of pouring of girder box by the RW method, its stress state is shown in the figure.

1. The maximum tensile stress of the CSWs along the bridge is 72 MPa, mainly located in the upper flange steel plate at the junction of the CSWs and top concrete. The maximum compressive stress is 124 MPa, mainly located in the lower flange steel plate at the junction of CSWs and bottom concrete.
2. The maximum vertical shear stress of the CSWs is 12 MPa, located at the action point of concentrated load. During the construction, the contact area should be appropriately enlarged when the hanging basket acts on the upper flange, and an eccentric load relative to the webs should not occur. The shear stress of the CSWs is about 5 MPa.

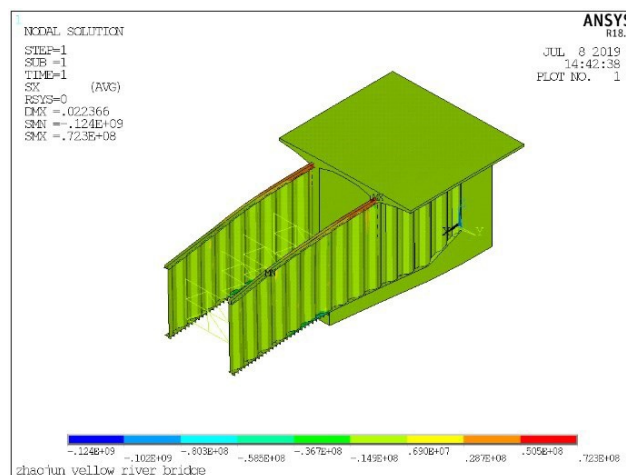


Fig. 8 Tensile stress of CSWs along the bridge. CSW, corrugated steel webs

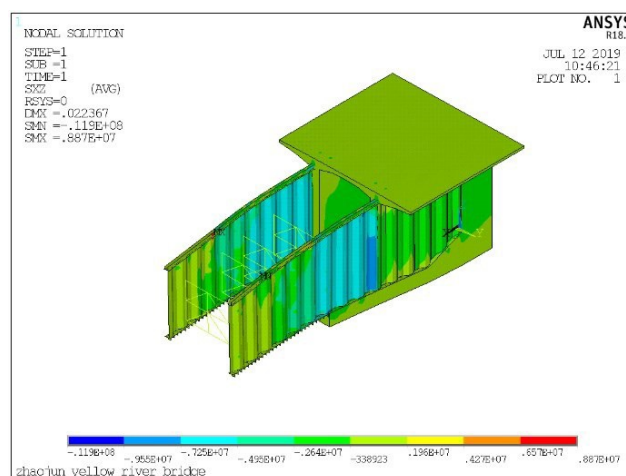


Fig. 9 Vertical shear stress of corrugated steel webs

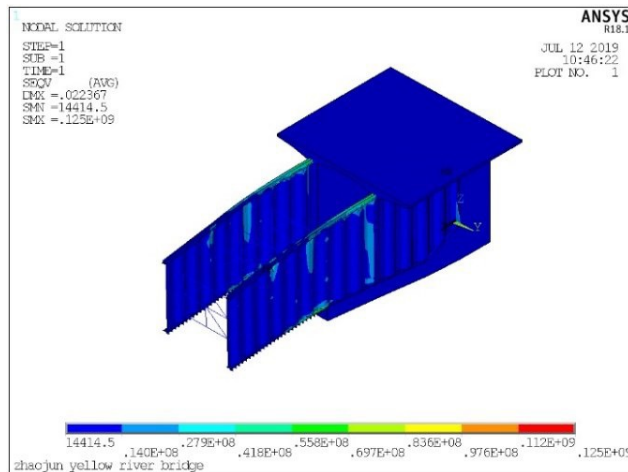


Fig. 10 Maximum equivalent stress of corrugated steel webs

3. The maximum equivalent stress (Mises stress) of the CSWs is 125 MPa, located at the junction of the lower flange steel plate of CSWs and 3# bottom concrete. It meets the requirements of the relevant design specification.

However, since the upper flange steel plate of the CSWs is welded to the CSWs, the welding quality must be guaranteed.

4.2 Stress Analysis of Top Concrete and Bottom Concrete

The analysis of the distribution of main stress on the top concrete indicates that 99% of the bottom concrete tensile stress is less than 1 MPa (or in the compressive state), in line with the requirements of the relevant design specifications. The stress concentration in concrete exists in the steel-concrete junction area of a 90° acute angle at the root of the 3# bottom concrete, with the maximum tensile stress of about 4 MPa. The excessive stress here is caused by the corner bending moment that is formed resultant to a tendency of separation between 3# bottom concrete and 2# lining concrete, which can in turn be attributed to the basket load and dead weight. It can be solved by strengthening the structural measures. When necessary, a (prestressed) tie rod can be added between the front cantilever of the 3# bottom concrete and the 2# top concrete to balance part of the load. The tensile stress of concrete at the steel-concrete junction area of the front part of 2# top concrete is about 4.5 MPa.

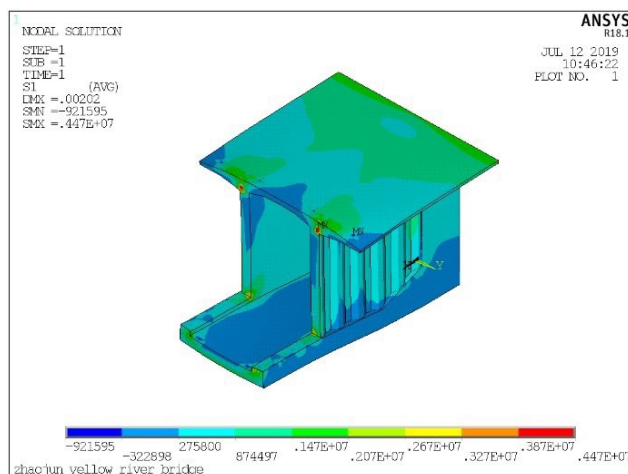


Fig. 11 Maximum equivalent stress of concrete slabs

Besides, the upper flange of the CSWs here is subjected to tension, generating a tensile effect on the concrete at the joint position and adding a cracking risk to the concrete. In fact, without adding the upper flange steel plate ‘π’ structure, the tensile stress of concrete here is about 6.5 MPa. During the actual construction, transverse bridge steel bars are installed here, which can further reduce the stress. As a result, we should properly arrange the structural reinforcement and ensure an optimal quality of construction during practical implementation of the model.

4.3 Stress Analysis of Lining Concrete

In practical engineering, horizontal and oblique cracks can easily occur in the lining concrete section of CSWs. In the Zhao-Jun Yellow River Super Large Bridge, coarse steel bars with JL32 finish rolling thread (area of the bar $S = (0.032/2)^2 \times \pi = 0.000804248 \text{ m}^2$) were used to apply the vertical pre-stress. The vertical prestressed steel bars were straight bars, the prestressed bars were replaced using the equivalent load method and the vertical prestressed load was given by: $S \cdot 0.9\text{FPK} = S \cdot 706.5 \text{ Mpa} = 568 \text{ kN}$.

As shown in figure, without considering the vertical prestressed bars, the lining concrete is generally subjected to tensile stress, and the red line area is correspondingly subjected to tensile stress. Therefore, there is a cracking risk to the lining concrete. However, when the vertical prestressed bars are considered, the lining concrete is basically in a compression state, which improves its stress state.

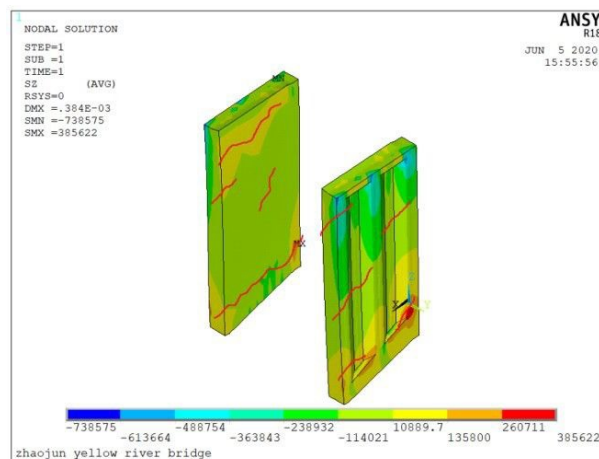


Fig. 12 Vertical stress of lining concrete without vertical prestressed bars

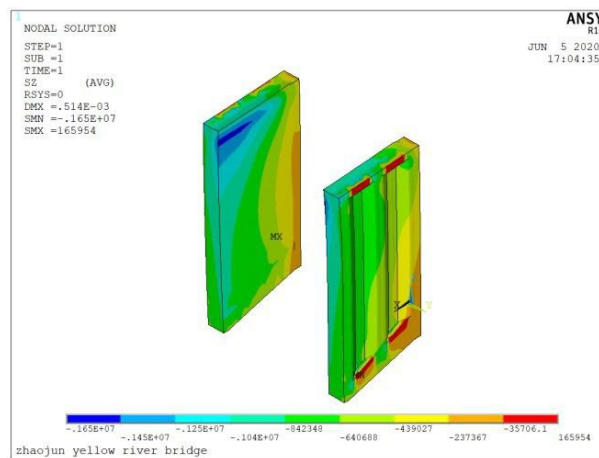


Fig. 13 Vertical stress of lining concrete with vertical prestressed bars

4.4 Stress Analysis of Temporary Support

The equivalent stress of temporary support is extracted, with the maximum tensile stress of 10.8 MPa. Therefore, the support is safe. A trial calculation of the stable critical stress of the compressive bar of the structure shows it is about 40,000 MPa. It is impossible for the structure to have such a large stress under the action of the hanging basket load, and it is thus free from the instability problem.

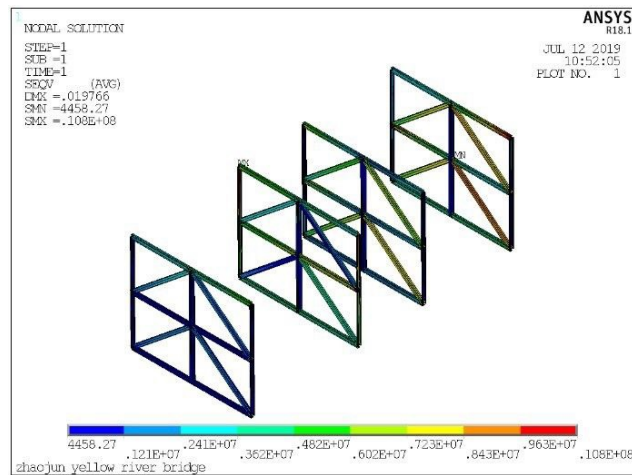


Fig. 14 Stress analysis of temporary support

5 Conclusion

1. During the cantilever construction by the RW method, the CSW was used as the bearing structure of hanging basket (or cantilever), and the pouring of top concrete and bottom concrete and the installation of CSWs were carried out in parallel, which can significantly shorten the construction period and improve the construction efficiency.
2. The results of the finite element simulative analysis provide the impression that during the cantilever construction using the RW method, the stress of CSWs was lower than that indicated in the standard design requirements, and that stress concentration occurred at the junction of the upper and lower flange steel plates and concrete with CSWs. Therefore, in practice, attention should be paid to the welding quality of CSWs and upper and lower flange steel plates, as well as the construction quality of the perforated steel plate, angle steel and structural steel bar at the junction.

Acknowledgements.

The research is sponsored by the Transportation Science and Technology Project of Inner Mongolia (Grant No. NJ-2018-10) and the academician special research funding projects of CCCC (Grant No. YSZX-02-2020-01-B).

References

- [1] Nie Jianguo, Tao Muxuan, WU Lili, NIE Xin, Li Faxiong, Lei Feilong. Advances of research on steel-concrete composite bridges [J]. China Civil Engineering Journal, 2012, 45(06):110-122.
- [2] Li Shuqin, Chen Jianbing, Wan Shui, Chen Huali. Application of the Pre-Stressed Concrete Box-Girder With Corrugated Steel Webs in Bridge Engineering in China [J]. Engineering Mechanics, 2009, 26(S1):115-118.

- [3] Gao Mingtian. Mechanical Analysis of Prestressed Concrete Composite Box. -Girdge Bridge with Corrugated Steel Webs for Multi-Working Plane Cantilever Casting Construction [D]. Southeast University, 2017.
- [4] Li Ning, Lu Yong, Chen Cheng, Jin Jin. Study on the Applicability of Cantilever Construction Technology by RW Method for Continuous Girder Bridge with Corrugated Steel Webs [J]. *Journal of China & Foreign Highway*, 2018, 38(01):145-147.
- [5] Li Hui, Chen Cheng, Liu Ningbo. Research and Application of Misalignment Method for Corrugated Steel Web [J]. *Construction Technology*, 2019, 48(03):66-69.
- [6] Jie Mingjun. Application of WR Method in Pre-stressed Concrete Box Girder Bridge with Corrugated Steel Webs [J]. *Railway Engineering*, 2017(04):45-47.
- [7] Jia Huijuan, Dai Hang, Zhang Jiandong. Research on Transverse Internal Forces in Box-Girder Bridges with Corrugated Steel Webs [J]. *Engineering Mechanics*, 2014, 31(12):76-82.
- [8] Ye Zhiwu, Luo Yongfeng, Chen Xiaoming, Jia Baorong. Improved Method of Step by Step Modelling and Its Application In Construction Simulation [J]. *Journal of Tongji University (Natural Science)*, 2016, 44(01):73-80.
- [9] Zheng Jiang, Ge Hongpeng, Wang Xiantie, He Zhen, Luo Yong. A method of element birth and death of local configuration constraint and its application in construction mechanics [J]. *Journal of Building Structures*, 2012, 33(08):101-108.